Ammonia in the UTLS: GLORIA airborne measurements for CAMS model evaluation in the Asian Monsoon and in biomass burning plumes above the South Atlantic

Sören Johansson[1], Michael Höpfner[1], Felix Friedl-Vallon[1], Norbert Glatthor[1], Thomas Gulde[1], Vincent Huijnen[2], Anne Kleinert[1], Erik Kretschmer[1], Guido Maucher[1], Tom Neubert[3], Hans Nordmeyer[1], Christof Piesch[1], Peter Preusse[4], Martin Riese[4], Björn-Martin Sinnhuber[1], Jörn Ungermann[4], Gerald Wetzel[1], and Wolfgang Woiwode[1]

[1]Institute of Meteorology and Climate Research - Atmospheric Trace Gases and Remote Sensing (IMK-ASF), Karlsruhe Institute of Technology, Karlsruhe, Germany
[2]R&D Weather and Climate models, Royal Netherlands Meteorological Institute (KNMI), De Bilt, Netherlands
[3]Central Institute of Engineering, Electronics and Analytics - Electronic Systems (ZEA-2), Forschungszentrum Jülich, Jülich, Germany
[4]Institute of Energy and Climate Research - Stratosphere (IEK-7), Forschungszentrum Jülich, Jülich, Germany

Correspondence: S. Johansson (soeren.johansson@kit.edu)

Abstract. Ammonia (NH_3) is the major alkaline species in the atmosphere and plays an important role in aerosol formation, which affects local air quality and the radiation budget. NH_3 in the Upper Troposphere and Lower Stratosphere (UTLS) is difficult to detect and only limited observations are available. We present two dimensional trace gas measurements of NH_3 obtained by the airborne infrared imaging limb sounder GLORIA (Gimballed Limb Observer for Radiance Imaging of the Atmosphere) that has been operated onboard the research aircraft Geophysica within the Asian Monsoon Anticyclone during the StratoClim campaign (July 2017) and onboard HALO (High Altitude and Long Range Research Aircraft) above the South Atlantic during the SouthTRAC campaign (September-November 2019). We compare these GLORIA measurements in the UTLS with results of the CAMS (Copernicus Atmosphere Monitoring Service) reanalysis and forecast model to evaluate its performance. The GLORIA observations reveal large enhancements of NH_3 of more than 1 ppbv in the Asian Monsoon upper troposphere, but no clear indication of NH_3 in biomass burning plumes in the upper troposphere above the South Atlantic above the instrument's detection limit of around 20 pptv. In contrast, CAMS reanalysis and forecast simulation results indicate strong enhancements of NH_3 in both measured scenarios. Comparisons of other retrieved pollution gases, such as peroxyacetyl nitrate (PAN), show the ability of CAMS models to generally reproduce the biomass burning plumes above the South Atlantic. However, NH_3 concentrations are largely overestimated by the CAMS models within these plumes. We suggest that emission strengths used by CAMS models are of lower accuracy for biomass burning in comparison to agricultural sources in the Asian Monsoon. Further, we suggest that loss processes of NH_3 during transport to the upper troposphere may be underestimated for the biomass burning cases above the South Atlantic. Since NH_3 is strongly undersampled, in particular at higher altitudes, we hope for regular vertically resolved measurements of NH_3 from the proposed CAIRT mission to strengthen our understanding of this important trace gas in the atmosphere.

1 Introduction

Ammonia (NH_3) is the major alkaline trace gas of the atmosphere and part of total reactive nitrogen. Sources of atmospheric NH_3 are livestock and fertilizer in agriculture, but also industry and combustion processes (e.g., Bouwman et al., 1997). Further, NH_3 has been measured in biomass burning plumes in vicinity of fires (e.g., Hegg et al., 1988; Coheur et al., 2007; Tomsche et al., 2023). It is expected that total emissions of NH_3 rise strongly, due to increased livestock, usage of fertilizers, and combustion (Szopa et al., 2021, and references therein). Atmospheric sinks of NH_3 are wash-out due to the high water solubility of NH_3, and formation of aerosols, like ammonium sulfate (in presence of sulfuric acid) or ammonium nitrate (in presence of nitric acid). The importance of NH_3 in the atmosphere for the initial formation of new particles has been corroborated by various studies (e.g., Kirkby et al., 2023, and references therein). As aerosols are of importance for local air quality, and for climate through their direct and indirect radiative impact (e.g., Szopa et al., 2021), it is necessary to observe and understand the distribution of NH_3 in the atmosphere from the boundary layer up to the lower stratosphere.

In situ measurements of NH_3 are, however, challenging due to the wide range of ambient levels (5 pptv to 500 ppbv) and the interaction of NH_3 with surfaces of the instrument ("sticky"; e.g., von Bobrutzki et al., 2010). Still, there are various in-situ measurements at boundary layer altitudes, but only very few in the free troposphere and very sparse measurements with high uncertainties in the upper troposphere (e.g., Ziereis and Arnold, 1986; Nowak et al., 2010; Tomsche et al., 2023) .

Due to its specific spectral lines in the thermal infrared region, remote sounding spectrometers are suited to quantify NH_3 in a "contact-free" manner. In that way, NH_3 has been observed by infrared sounders from satellite and aircraft in nadir and limb geometry. From satellite instruments measuring in nadir, such as TES (Tropospheric Emission Spectrometer), IASI (Infrared Atmospheric Sounding Interferometer), CrIS (Cross-track Infrared Sounder), or AIRS (Atmospheric Infrared Sounder), global observations of NH_3 in the lower troposphere are available (e.g., Beer et al., 2008; Clarisse et al., 2010; van Damme et al., 2015; Shephard and Cady-Pereira, 2015; Warner et al., 2016). First observations of NH_3 in the upper troposphere (in particular of the Asian summer monsoon) have been achieved by the MIPAS (Michelson Interferometer for Passive Atmospheric Sounding) instrument from the Envisat satellite (Höpfner et al., 2016), and by the GLORIA (Gimballed Limb Observer for Radiance Imaging of the Atmosphere) instrument onboard the Geophysica research aircraft (Höpfner et al., 2019). The connection of large amounts of NH_3 reaching the upper troposphere through convection with the formation of solid ammonium nitrate (AN) particles as secondary aerosols was also shown during these flights (Höpfner et al., 2019; Wagner et al., 2020; Appel et al., 2022).

In the present work, we utilize observations of mid- to upper tropospheric NH_3 obtained within two aircraft campaigns of the GLORIA instrument, to evaluate the ability of the CAMS atmospheric model to describe the distribution of NH_3 under two different scenarios: within the Asian summer monsoon and within biomass burning plumes. Beside the direct comparison of NH_3, we further use peroxyacetyl nitrate (PAN) as a long-lived ($\tau \approx 3$ months) pollution tracer, which has been shown to be useful to identify biomass burning plumes in GLORIA and CAMS data (e.g. Johansson et al., 2022).
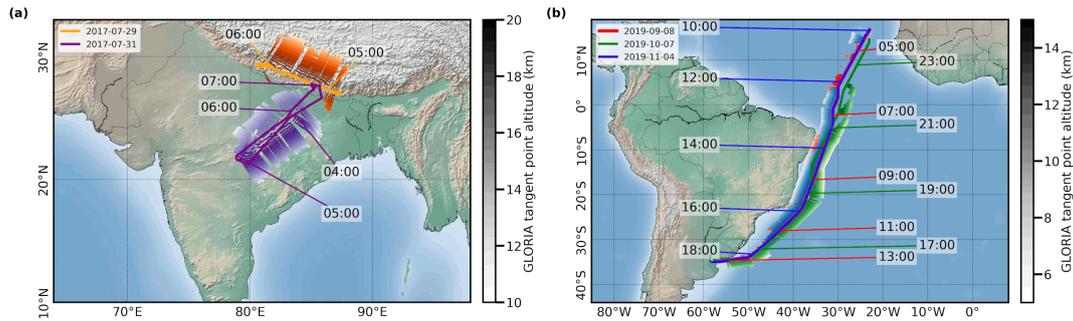
Figure 1. Flight paths and locations of GLORIA tangent points for discussed flights of (a) the StratoClim campaign and (b) the SouthTRAC campaign. Tangent points affected by clouds are not used in the retrieval process and result in gaps in the plotted geolocations. Note different color bar ranges and map scales for each panel. The flight path of the flight on 8 September 2019 is identical to the flight path of the flight on 4 November 2019, which hides large parts of the earlier flight.

2 Observations and atmospheric model simulations

2.1 GLORIA measurements

The GLORIA instrument has been deployed on various airborne campaigns with the M55 Geophysica and the HALO research
55 aircraft. In this study, GLORIA measurements from the M55 Geophysica StratoClim campaign (July/August 2017, base in
Kathmandu, Nepal), and from the HALO SouthTRAC campaign (September-November 2019 with bases in Oberpfaffenhofen,
Germany and Rio Grande, Argentina) are discussed. Flight paths and the location of GLORIA tangent points are summarized
in Fig. 1. For this study, StratoClim flights on 29 July 2017 and 31 July 2017 have been selected because of measured high
NH_3 (Höpfner et al., 2019), while SouthTRAC flights on 8 September 2019, 7 October 2019, and 4 November 2019 are chosen
60 because of measured large pollution plumes above the South Atlantic (Johansson et al., 2022). Both StratoClim flights were
conducted from and to Kathmandu, Nepal, and the three selected SouthTRAC flights were directed from Sal, Cape Verde, to
Buenos Aires, Argentina, and vice versa, as part of the transfer flights between Germany and Argentina.

The GLORIA instrument (Friedl-Vallon et al., 2014; Riese et al., 2014) combines an imaging detector working in the
thermal infrared with a Fourier-Transform-Spectrometer in an actively controlled gimbal frame. This combination allows for
65 simultaneous observations of 128×48 (vertical $\times$ horizontal) atmospheric spectra, high spectral sampling up to 0.0625 cm^{-1},
and compensation of aircraft movements and active targeted line-of-sight control. Further, two external black bodies are used
for in-flight radiometric calibration measurements, together with upward looking atmospheric "deep space" observations. For
the measurements discussed in this work, interferograms which were obtained with a maximum optical path difference (MOPD)
of 8.0 cm (spectral sampling of 0.0625 cm^{-1}) are used. Only during the StratoClim flight on 29 July 2017, due to operational
70 restrictions, interferograms with 2.5 cm MOPD were recorded, resulting in a spectral sampling of 0.2 cm^{-1}. Within GLORIA
level 1 processing, the interferograms are Fourier-Transformed and radiometrically and spectrally calibrated. The resulting
calibrated spectra at each detector pixel are screened, filtered, and finally horizontally binned into 127 spectra per recorded

measurement sampled in the vertical direction (with one horizontal line of spectra beeing disregarded completely due to detector artifacts; Kleinert et al., 2014; Ungermann et al., 2022). All GLORIA retrievals in this study are based on version v03.02 of GLORIA level 1 data (calibrated spectral radiances).

Based on these binned calibrated spectra, profiles of atmospheric temperature and trace gases are retrieved perpendicular to the flight track (Johansson et al., 2018). The retrieval uses a nonlinear least-squares fit with Tikhonov regularization of the retrieval software KOPRAFIT together with the radiative transfer model KOPRA (Stiller, 2000). For NH_3, the overall retrieval strategy from Höpfner et al. (2019) is applied, for PAN, retrievals as described by Johansson et al. (2020, 2022) are utilized, and for AN, retrievals as described by Höpfner et al. (2019). Due to the reduced spectral sampling on the flight of 29 July 2017, spectral windows and regularization have been adjusted slightly (see supplementary Tab. S1). For NH_3 retrievals of StratoClim flights, vertical resolutions between 0.8 and 1.3 km, and estimated errors between 10 and 50 pptv have been achieved, for SouthTRAC flights discussed in this work, vertical resolutions between 0.5 and 0.7 km, and estimated errors between 6 and 12 pptv (10,90 percentile ranges, each).

In addition, for cloud information, the so-called cloud index is calculated as a ratio of spectral windows (see Spang et al., 2004). Please note that lower cloud index values mean a higher contamination of clouds along the line of sight.

2.2 CAMS global atmospheric composition model configurations

As part of the Copernicus Atmosphere Monitoring Service (CAMS), two data products are publicly available: First, the ECMWF (European Centre for Medium-Range Weather Forecast) Atmospheric Composition Reanalysis version 4 (EAC4; Flemming et al., 2015; Inness et al., 2019), and second, the CAMS global atmospheric composition operational near-real time forecasts. Both atmospheric model configurations use the ECMWF Integrated Forecast System (IFS) model, and assimilate multiple observations of atmospheric state and composition. In this study, CAMS model output is linearly interpolated in space and time onto GLORIA measurement geolocations to ensure optimal comparisons between observation and model output.

For this work, we compare GLORIA data to both CAMS configurations to achieve two goals: First, we want to compare GLORIA NH_3 obtained during two different campaigns 2017 and 2019 with a consistent data set that did not change for the time ranges of both campaigns. For this purpose, the reanalysis configuration is suited best. Second, we want to compare GLORIA NH_3 to the most recent CAMS configuration that is publicly available, which is the CAMS forecast configuration, in order to check for improvements for more recent model versions.

2.2.1 CAMS reanalysis

The CAMS reanalysis is currently available between 2003 and 2021, uses 60 vertical levels between 0.1 and 1000 hPa, and a horizontal resolution of $0.75° \times 0.75°$ latitude $\times$ longitude. Data is provided every 3 h and includes meteorological parameters, concentrations of chemical trace gases, as well as aerosols. It is based on IFS cycle 42r1, and employs data assimilation of trace gases O_3, CO, and NO_2, along with aerosol optical depth (Inness et al., 2019). Chemistry is handled by a module named IFS(CB05) (Flemming et al., 2015), with its tropospheric chemistry as inherited from the TM5 model (Huijnen et al., 2010), and aerosols are treated as described by Morcrette et al. (2009). Anthropogenic emissions are prescribed from MACCity

(MACC/CityZEN; Granier et al., 2011), biogenic emissions from MEGAN2.1 (Model of Emissions of Gases and Aerosols from Nature; Guenther et al., 2012), and biomass burning emissions from GFAS v1.2 (Global Fire Assimilation System; Kaiser et al., 2012). CAMS reanalysis has been evaluated by various aircraft measurements: Wang et al. (2020) compared tropospheric trace gas profiles over the Arctic, North America, and Hawaii to CAMS reanalysis and show that simulated PAN is in agreement with observations. Further, Johansson et al. (2020, 2022), and Wetzel et al. (2021) compared GLORIA PAN and other pollution trace gases to CAMS reanalysis data in the upper troposphere above the Asian Monsoon, the North Atlantic, and the South Atlantic, respectively. They found an overall agreement for the measured plume structures and for biomass burning plumes above the South Atlantic (including SouthTRAC flights that are discussed in this study). In these plumes especially the trace gas PAN was even in quantitative terms described well by the model. To our knowledge, there are no studies available evaluating NH_3 for CAMS reanalysis. However, since NH_3 and PAN can be emitted both from biomass burning events, it is important to know that CAMS is able to reproduce biomass burning PAN plumes.

2.2.2 CAMS forecast

The CAMS global atmospheric composition near-real time forecast is operationally available since 2015, and in contrast to the reanalysis, this data product receives a version upgrade approximately once a year. For this reason, the CAMS forecast data for StratoClim measurements in 2017 (cycle 43r1) are different to those for SouthTRAC measurements in 2019 (cycle 46r1). Both forecast model results are based on a newer model version compared to CAMS reanalysis (cycle 42r1). The model utilizes 60 vertical levels for simulations for 2017, and 137 model levels for 2019, and in both cases a horizontal resolution of $0.4° \times 0.4°$ latitude $\times$ longitude. New forecasts are started every day at 0:00 UTC and 12:00 UTC, and output is provided every 3 h for vertically resolved parameters. In this work, model output of shortest possible lead times of 0, 3, 6, and 9 h are used for interpolation as mentioned above.

Besides changes in resolution, CAMS forecast for the measurements in 2017 differs compared to CAMS reanalysis, among other things in the following aspects: Additional observational data sets are considered for assimilation (e.g., vertical ozone profiles of the Ozone Mapping and Profiler Suite). Further, a new source scheme for Secondary Organic Aerosols, which is based on scaled CO emissions, is introduced (Eskes et al., 2016). Additionally, CAMS forecasts for the measurements in 2019 differs among other things in these aspects: Now, CAMS makes use of `CAMS_GLOB_ANT` v2.1 anthropogenic and `CAMS_GLOB_BIO` v1.1 biogenic emissions. Biomass burning plume injection height from GFAS is introduced, along with a diurnal cycle in its emissions. Further, separate ammonium and nitrate aerosol species are introduced, interaction between chemistry and aerosol schemes are established, which implied a change in the modelled NH_3 life cycle. Also a selection of chemical reaction rates are updated (Eskes et al., 2017, 2018; Basart et al., 2019).

In order to compare CAMS forecast ammonium aerosol to GLORIA AN, the CAMS ammonium aerosol mass mixing ratio is scaled according to the molar mass ratio of ammonium nitrate to ammonium, and then converted to mass density. This approach may overestimate AN if not all of the ammonium aerosol in the model is present in the form of AN.

3 Ammonia measurements and comparisons

In this section, GLORIA measurements of NH$_3$ are presented and compared to CAMS reanalysis and forecast simulation results. In addition, as indicator for the pollution plumes, GLORIA measurements of PAN are shown. First, the two flights from the StratoClim campaign within the Asian monsoon air are presented, followed by three SouthTRAC flights concentrating on biomass-burning situations.

3.1 Asian Monsoon

From space-borne infrared nadir and limb-observations it is known that elevated concentrations of NH$_3$ are present in the atmosphere above the Indian subcontinent at lower levels (van Damme et al., 2015) and even in the upper troposphere during the time of the Asian Monsoon (Höpfner et al., 2016). For the GLORIA airborne measurements on 31 July 2017, strongly enhanced abundances of NH$_3$ of up to about 1000 pptv were reported (Höpfner et al., 2019). The current analysis of the flight on 29 July 2017 above Nepal shows even higher concentrations of up to 1500 pptv, as presented in Fig. 2a. This maximum is part of a larger horizontal structure between 5:30 UTC and 6:15 UTC and 12 km to 14 km altitude. Peak values of NH$_3$ VMRs coincide with maximum PAN VMRs (Fig. 2d). CAMS reanalysis (Fig. 2b) indicates a similar NH$_3$ enhancement at the same altitude range, but shifted to earlier measurement times (eastwards). In addition, a thin maximum up to 700 pptv NH$_3$ is present at 15 km altitude, which is at a similar location as a second, smaller observed PAN maximum (see Fig. 2d), but does not correspond to a measured NH$_3$ maximum. CAMS forecast also shows two plumes, but spatially shifted and of different intensity. This model indicates a major NH$_3$ maximum around 6:00 UTC peaking at approximately 14 km altitude. Maximum VMRs are up to 900 pptv and thus smaller than observed, which may be caused by too fast NH$_4^+$ production in the model. Another maximum is forecasted at approximately 05:30 UTC and 12 to 16 km altitude with maximum VMRs up to 1000 pptv at 12 km altitude.

The StratoClim flight on 31 July 2017 reveals one large enhancement of NH$_3$, peaking at 4:15 UTC and 14 km altitude with VMRs up to 1000 pptv (Fig. 3a). A second, faint maximum (4:30-4:50 UTC, 12 km altitude) indicates lower VMRs up to 100 pptv. For the second part of the flight (later than 5:00 UTC), GLORIA measurements show no enhanced NH$_3$. This contrast in NH$_3$ distributions between both parts of the flight is remarkable, since the flight region of the second part of the flight is relatively close to the flight region of the first part of the flight, and mainly the viewing direction of GLORIA has changed from south-eastward to north-westward (see Fig. 1a). Hence, our GLORIA measurements indicate strong horizontal variability of NH$_3$ in the Asian Monsoon upper troposphere. However, PAN observations indicate polluted air masses also for this second part of the flight. These PAN pollution plumes in the second part of the flight are reproduced by CAMS reanalysis and forecast (see Johansson et al., 2020 and supplementary Fig. S1 and Fig. S2). CAMS reanalysis and forecast successfully reproduce the approximate position of the observed NH$_3$ plumes, as well as the absence of NH$_3$ plumes in the second part of the flight (see Fig. 3b,c). However, CAMS reanalysis does not simulate the major plume later than 4:10 UTC, and also maximum VMRs are simulated below 400 pptv, and thus considerably lower than the measured ones. CAMS forecast also simulates the largest VMRs of the major plume earlier than measured, but maximum VMRs are comparable to the GLORIA measurements.
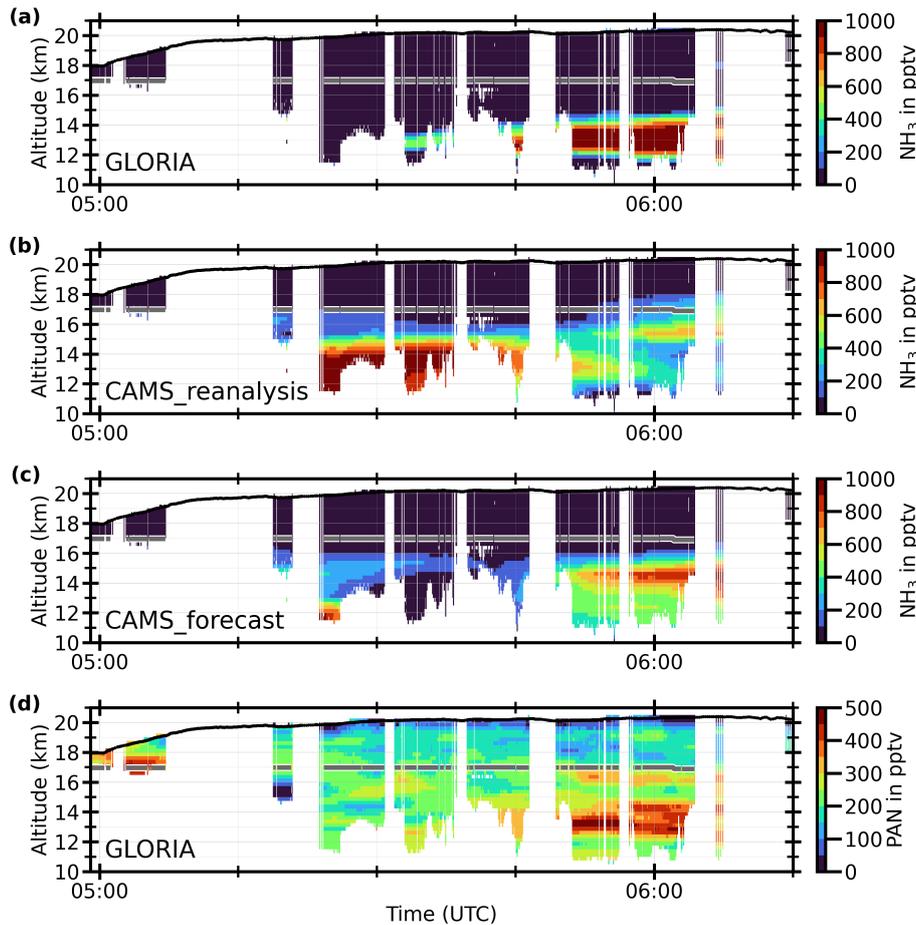
Figure 2. StratoClim flight on 29 July 2017 from and to Kathmandu, Nepal: GLORIA time/altitude cross sections of (a) NH$_3$ and (d) PAN together with CAMS reanalysis (b) and CAMS forecast (c) simulation results, interpolated onto GLORIA geolocations. GLORIA data is horizontally averaged to match lower horizontal resolutions of CAMS forecast of $\approx$44 km. The black line indicates flight altitudes, the gray line shows the ECMWF analysis 380 K potential temperature as indication of the tropopause location in the Asian Monsoon. Blank spaces indicate regions of high cloud tops, calibration measurements, or aircraft movements (like curves). Maximum NH$_3$ VMRs are measured up to 1500 pptv and thus exceed color bar maximum.

3.2 Biomass burning plumes above the South Atlantic

All three of the transfer flights between Sal, Cape Verde, and Buenos Aires, Argentina, and vice versa, have been influenced by pollution plumes, originating from biomass burning events (Johansson et al., 2022). In the following we will discuss the observations of NH$_3$ by GLORIA within these plumes in comparison to both CAMS reanalysis and forecast model configurations.

175   For the SouthTRAC flight on 8 September 2019 (Fig. 4a), GLORIA measured less than 20 pptv NH$_3$ over large parts of the flight, despite clear biomass burning plume structures observed in PAN (Fig. 4d). Very small enhancements below 60 pptv
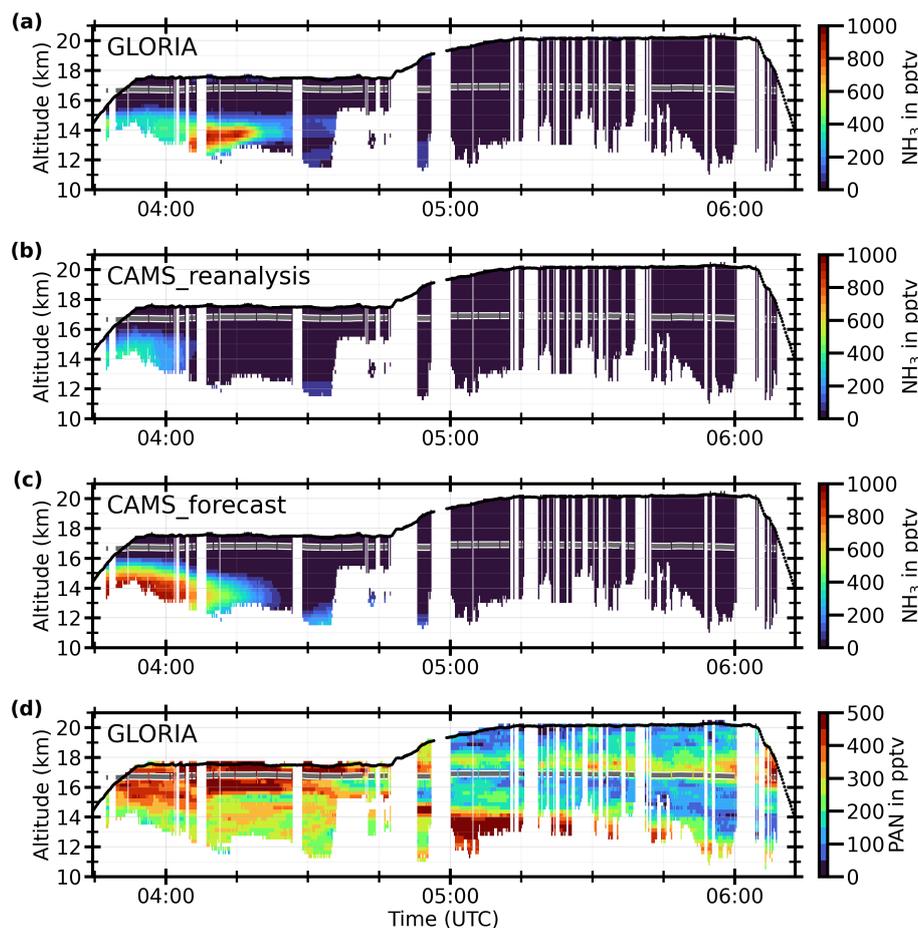
Figure 3. Same as Fig. 2, but for flight on 31 July 2017. Maximum NH$_3$ VMRs are measured up to 1100 pptv and thus exceed color bar maximum.

are indicated at approximately 10:15 UTC and 13 km altitude, surrounding the filtered air masses, where no retrieval has been possible due to cloud or aerosol contamination. In such close proximity, the cloud or aerosol feature, however, could have affected the NH$_3$ retrieval quality. CAMS reanalysis (Fig. 4b) and forecast (Fig. 4c) simulate enhanced concentrations of NH$_3$

180   within extended areas, which are correlated with the PAN biomass burning plumes. CAMS reanalysis shows two horizontal plumes with VMRs up to 250 pptv, between 9:30 and 11:00 UTC and at 8 and 11 km altitude. This structure corresponds to the measured biomass burning plumes. Using backward trajectories, it has been shown that these air masses likely entered the upper troposphere above central South America (see Fig. 3 of Johansson et al., 2022), while other air masses with enhanced PAN originated from Africa. Further, GLORIA measured C$_2$H$_4$ (upper tropospheric life time of $\approx$1.2 d) exclusively at these

185   spots, which indicates a young age of these air masses (see Fig. 1 of Johansson et al., 2022). Similarly, CAMS forecast indicates maximum VMRs up to 400 pptv for these plumes. In addition, CAMS forecast also simulates enhancements of lower VMRs up
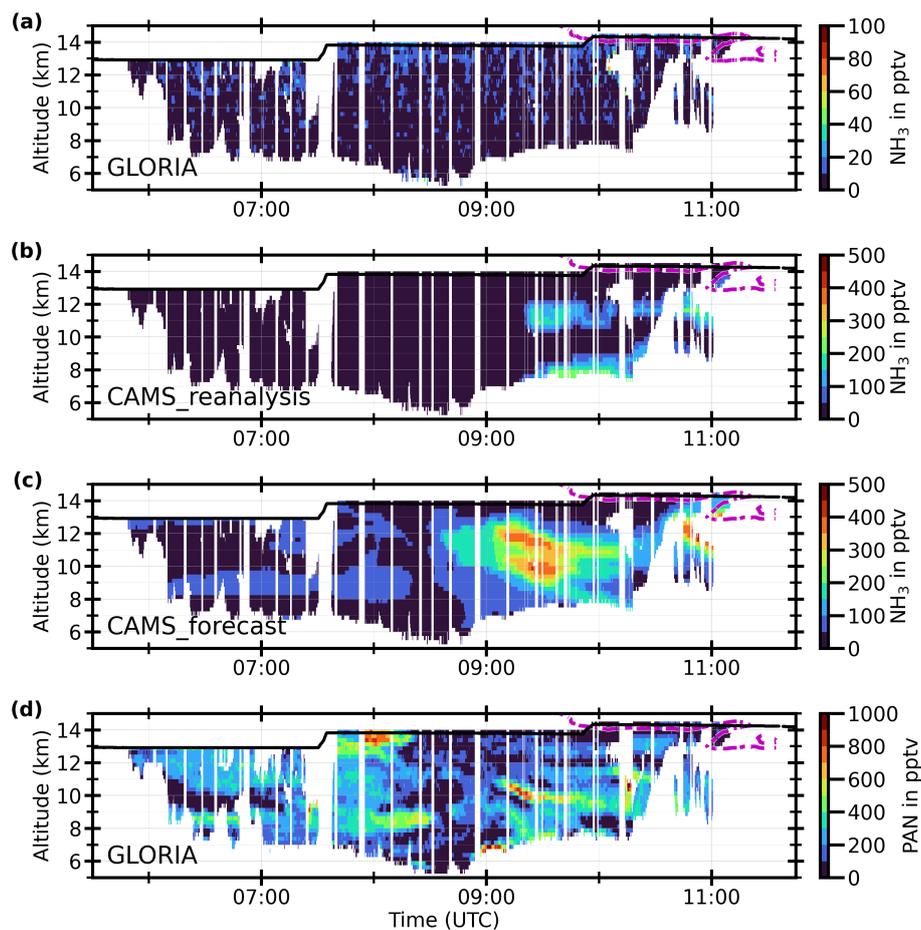
Figure 4. SouthTRAC flight on 8 September 2019 from Sal, Cape Verde, to Buenos Aires, Argentina: GLORIA time/altitude cross sections of (a) NH_3 and (d) PAN together with CAMS reanalysis (b) and CAMS forecast (c) simulation results, interpolated onto GLORIA geolocations. GLORIA data is horizontally averaged to match lower horizontal resolutions of CAMS forecast of ≈ 44 km. The black line indicates flight altitudes, the dashed magenta line shows the ECMWF $\pm 2, 4$ PVU isolines as indication of the tropopause. Due to tropopause heights, which are partially located above flight altitude, these magenta lines are not always present, and sometimes only the ± 2 PVU line is present. Blank spaces indicate regions of high cloud tops, calibration measurements, or aircraft movements. Note that color bars for NH_3 change between GLORIA measurements (a) and both CAMS simulation results (b-c). Further, color bars have been adjusted to generally lower NH_3 VMRs compared to Figs. 2-3.

to 100 pptv for air masses associated with PAN plumes in the first part of the flight (e.g., 6:15 to 8:30 UTC and 9 km altitude, and 8:00 UTC and 12 km altitude). No similar enhancements of NH_3 are visible in the GLORIA observations.

The SouthTRAC flight on 7 October 2019 was characterized by a large, nose-like plume of PAN (and other pollution species) with high VMRs up to 1000 pptv (17:30 to 20:15 UTC, and 8 to 12 km altitude; Fig. 5d). This plume is reproduced by both CAMS model configurations, and trajectories indicate central South America as source of these air masses (see Johansson

190
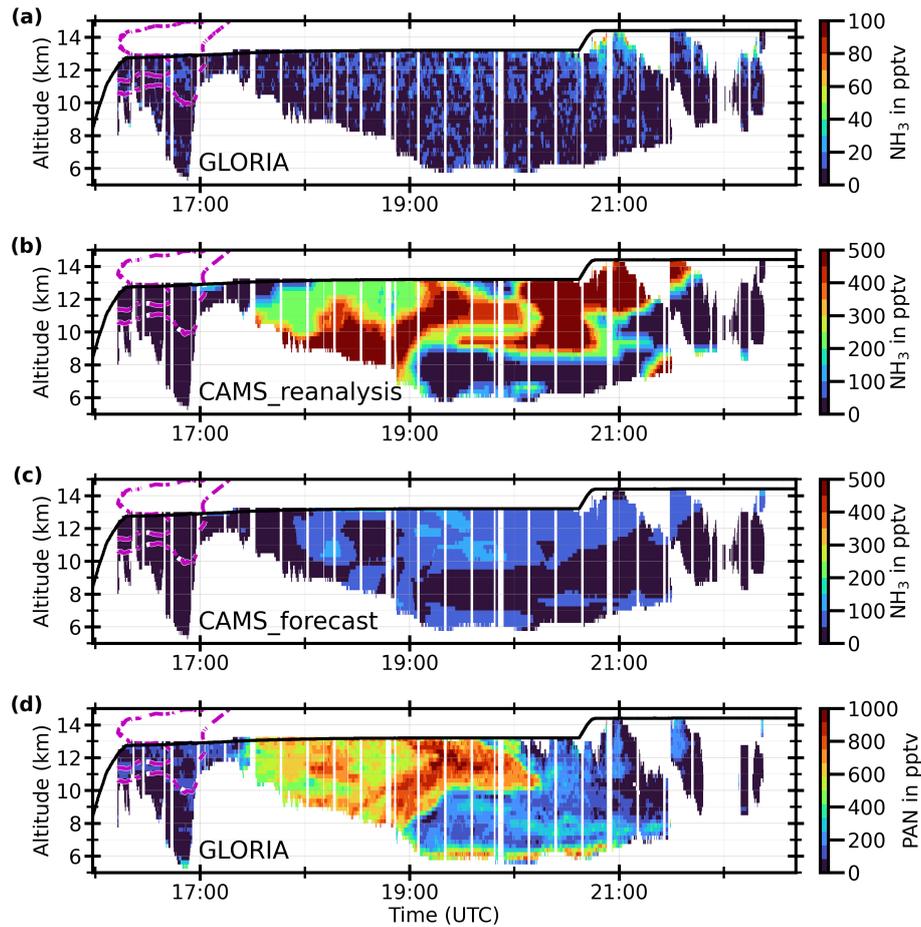
Figure 5. Same as Fig. 4, but for flight on 7 October 2019 from Buenos Aires, Argentina, to Sal, Cape Verde.

et al., 2022 and supplementary figures). Further, background PAN VMRs between 19:00 and 21:00 UTC are up to 350 pptv and thus considerably larger than tropospheric background concentrations in the beginning of the flight, which indicates further pollution outside the major PAN plume. NH_3 as measured by GLORIA (Fig. 5a), does not show any plume-like structure, but

195 background VMRs below 30 pptv. Again, close to a possible aerosol or cloud contamination at 21:00 UTC and 13 km altitude, larger NH_3 VMRs up to 70 pptv are observed. As mentioned for measurements of SouthTRAC flight on 8 September 2019, this NH_3 enhancement might be an artifact due to the challenging conditions for the retrieval in the presence of clouds and aerosols.

In contrast to the observations, the CAMS reanalysis simulates large amounts of NH_3 of more than 1500 pptv. Parts of the

200 simulated NH_3 plume resemble the large nose-like PAN plume, as measured by GLORIA. Other parts of the plume include the air masses of the elevated background PAN VMRs, and also the region of enhanced measured NH_3, but more than an order of magnitude higher than observed. The CAMS forecast does not simulate as high NH_3 VMRs as the reanalysis, but
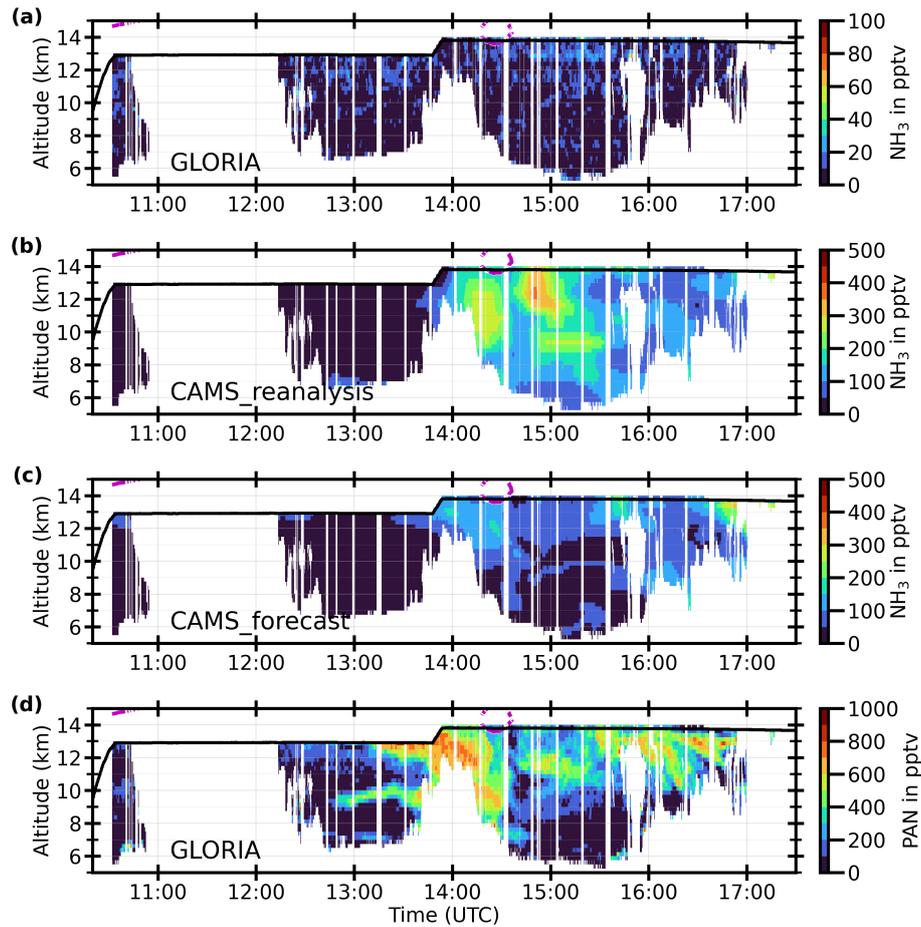
Figure 6. Same as Fig. 4, but for flight on 4 November 2019 from Sal, Cape Verde, to Buenos Aires, Argentina.

still maximum VMRs up to 150 pptv, which is considerably more than measured by GLORIA. The structure of maximum simulated NH_3 VMRs coincides with measured PAN maxima and thus indicates that the CAMS forecast also simulates large 205 NH_3 VMRs within biomass burning plumes.

Similar to both presented SouthTRAC flights, the GLORIA observations on 4 November 2019 do not show enhanced NH_3 concentrations, despite PAN plumes measured in these air masses (see Fig. 6a,d). Between 14:30 and 16:00 UTC, small enhancements of NH_3 are observed at 13 km altitude, just below flight altitude. Otherwise, NH_3 VMRs are below 20 pptv. Again, CAMS reanalysis and forecast largely overestimate NH_3 for this flight: CAMS reanalysis (Fig. 6b) simulates up to 210 400 pptv of NH_3 at measurement times with enhanced PAN observations. However, simulated NH_3 structures are not directly comparable to the observed PAN distributions. Still, simulated PAN patterns, in particular at 15:00 UTC, are similar to this NH_3 distribution (see supplementary Fig. S5). This indicates an overall displacement of the simulated plumes compared to the

GLORIA observations. CAMS forecast (Fig. 6c) again shows lower NH_3 concentrations compared to the reanalysis, but still values of up to 150 pptv. In this case, simulated NH_3 patterns resemble more the structures observed in PAN.

215 ## 3.3 Discussion

The GLORIA NH_3 observations show very different situations for the atmosphere above the Asian Monsoon and above the South Atlantic. While GLORIA measured plumes of strongly enhanced NH_3 VMRs in the upper troposphere within the Asian summer Monsoon, biomass burning plumes above the South Atlantic do not show detectable enhancements of NH_3. Comparisons with both CAMS models for the StratoClim measurements during the Asian monsoon show reasonable agreement

220 in quantitative terms as well as in the location of the plumes (within the expected performance of the model). In particular the better representation of the major plume during the flight on 31 July 2017 in the CAMS forecast (compared to the CAMS reanalysis) may be due to the higher horizontal resolution and upgraded model properties of the forecast (see Sec. 2.2.2).

For the SouthTRAC flights above the South Atlantic, CAMS reanalysis and forecast both simulate NH_3 plumes of several hundred pptv, which are correlated with biomass burning plumes, but which are not observed by GLORIA. The simulated

225 biomass burning plumes (in particular the PAN plumes) show reasonable agreement with the GLORIA PAN measurements, which excludes a mismatch of the plume locations between model and observation as reason for the disagreement in NH_3. In particular, the spatial resolution employed by CAMS has shown to be useful to reproduce the biomass burning plumes that are discussed in this work.

This difference in the ability of CAMS models to reproduce measured NH_3 VMRs may have various reasons: Sources for

230 NH_3 may be of different quality for different regions on Earth and also for different emission types. While the enhancements of NH_3 measured in the Asian Monsoon on 31 July 2017 likely stem from anthropogenic (agricultural) activities (see Supplementary figures 10-11 of Höpfner et al., 2019), plumes above the South Atlantic, in which CAMS models show enhanced NH_3, are likely to come from biomass burning events, as it was shown by (Johansson et al., 2022) by employing backward trajectories and analyses of different pollutants for these air masses. These two types of emissions, anthropogenic and biomass

235 burning, are prescribed by different emission data sets in CAMS model simulations (see Sec. 2.2), and both data sets may vary in their accuracy and precision regarding NH_3.

When comparing the amount of NH_3 in the lower atmosphere near the surface (Supplementary figures S6-S7), the CAMS reanalysis dataset shows comparable values in the order of 10 ppbv in the Asian Monsoon over Northern India/Pakistan by end of July 2017 as well as over the burning regions in the Amazonian in October 2019. The concentrations in the Monsoon

240 region are in broad agreement with the total column amounts of NH_3 as observed by IASI (Clarisse et al., 2023). Regarding the biomass-burning cases, the near-surface concentrations of the model appears consistent with observations of NH_3 within fire plumes of tens to few hundreds of ppbv (Tomsche et al., 2023). However, IASI total column amounts in the region of the South American plume-origin in autumn 2019 are by a factor of around 5 less abundant compared to the ones inside the monsoon. This would indicate an overestimation of the model with respect to the Amazonian fire sources. In addition, NH_3 emissions

245 of fire plumes are highly variable and strongly depend on factors such as fire size, soil composition, fuel composition, or fire weather (e.g., Tomsche et al., 2023).

Further, atmospheric sinks, such as wet deposition or formation of ammonium (NH_4^+)-containing aerosols, may be underestimated by CAMS model configurations within biomass burning plumes above the South Atlantic. In order to evaluate the ability of the model to reproduce the formation of NH_4^+ aerosols, we compared the GLORIA AN for the SouthTRAC flights with CAMS forecast ammonium aerosol (Supplementary figures S8-S10). Similar to the NH_3 comparisons, AN is not notably enhanced in the GLORIA measurements (beside small enhancements, which correlate with enhanced cloud contamination), but it is considerably enhanced in CAMS forecast. Since the formation of AN is expected to happen in the upper troposphere, the absence of AN in GLORIA data, together with the presence of AN in CAMS forecast suggest that the model already transported too much NH_3 into the upper troposphere for the biomass burning plumes. This overestimation of AN is in line with recent comparisons of different CAMS model configurations, where older configurations (such as the 2019 CAMS forecast configuration) tend to overestimate ammonium (Rémy et al., 2024).

In order to find hints of missing wet deposition, GLORIA cloud index is compared to CAMS forecast cloud fraction (Supplementary figures S8-S10). For all three examined SouthTRAC flights it seems like the model underestimates the presence of clouds in the measured air masses. However, this comparison is potentially misleading, since the GLORIA cloud index could potentially be influenced by aerosols, or by clouds, which are along the line of sight, but not necessarily on the tangent point, on which the CAMS forecast cloud fraction was sampled.

In addition, it is still under discussion, how NH_3 is efficiently transported into the upper troposphere in the Asian Monsoon without being washed-out by the strong precipitation within thunderstorms. For example, Ge et al. (2018) explain large NH_3 VMRs by deep convective vertical transport of NH_3 being dissolved in liquid cloud droplets, from which NH_3 would be released during the freezing process of the cloud particles. However, this transport mechanism may be imitated by the CAMS models by a lower wash-out, which is helpful for the Asian Monsoon, but not for biomass burning above the South Atlantic.

4 Conclusions

In this work, we have tested different CAMS model configurations with respect to their capability to simulate NH_3 mixing ratios in the upper troposphere. Knowledge about NH_3 in the atmosphere is important due to the influence of NH_3 on aerosol formation in an altitude region strongly influencing Earth's radiative budget.

We have selected two general scenarios, where enhanced concentrations of NH_3 can be expected to be transported from ground sources to high altitudes: the Asian monsoon, and strong biomass burning in South America and Africa. In both cases, the CAMS model configurations simulated elevated amounts of NH_3 in the upper troposphere.

Comparing these model data with observation of NH_3 obtained by the GLORIA infrared remote sounding instrument during two aircraft measurement campaigns reveals that the model configurations reproduce broadly well the observations of elevated NH_3 concentrations within the Asian summer monsoon. However, they strongly overestimate NH_3 within the biomass burning plumes in the mid-upper tropical troposphere, where no clear enhancement is visible in our measurements.

Clarifying the reason for this model overestimation is beyond the scope our analysis. However, we suggest that the emission of NH_3 through biomass burning might be overestimated. It is known that NH_3 emissions are challenging to simulate due to

280 its large variability, which is among others influenced by fire size, soil and fuel composition, and fire weather. Still there exist large uncertainties about the losses of NH_3 through different processes like particle formation and wash-out on its way from its source region to the measurement location in the upper troposphere. By comparing measurements of GLORIA AN with an estimation of CAMS forecast AN, we suggest that conversion of NH_3 into AN is not responsible for the overestimation of NH_3 by the model.

285 In terms of measurements, NH_3 is strongly undersampled especially at higher altitudes of our atmosphere, which means that there is a need for more vertically resolved observations. Here we have shown, that by using vertically high resolved observation from spectroscopic infrared limb-observations, it is possible to judge on the skills of atmospheric models to describe this trace gas correctly. With hopefully upcoming satellite missions, like ESA's Earth explorer 11 candidate CAIRT (Changing-Atmosphere Infra-Red Tomography Explorer; Sinnhuber et al., 2023), it will be possible to get daily global and altitude-
290 resolved vertical distribution of NH_3 from the mid-troposphere to the lower stratosphere. In combination with infrared nadir sounders, like IASI, it will be possible to gain much more insight in the processes governing the distribution of NH_3 in our atmosphere.

Data availability. GLORIA measurements are available in the database HALO-DB (https://halo-db.pa.op.dlr.de/mission/101 and https://halo-db.pa.op.dlr.de/mission/116) and will be available on the KITopen repository (https://doi.org/10.5445/IR/1000170770). The CAMS
295 model data is available from the Copernicus Atmosphere Data Store (https://ads.atmosphere.copernicus.eu). IASI NH_3 v4 columns are available online: https://iasi.aeris-data.fr/NH3/

Author contributions. SJ initiated the study, performed the analyses, and wrote the manuscript together with MH. GW, MH, JU, AK, NG, PP, and SJ performed the GLORIA data processing. FFV, EK, TG, CP, GM, HN, TN and coworkers operated GLORIA during the StratoClim and SouthTRAC campaigns. MH, MR, JU, BMS, WW and SJ participated in scientific flight planning during the campaigns. VH provided
300 insights into the CAMS simulations. All authors commented on and improved the manuscript.

Competing interests. The authors declare that they have no conflict of interest.

Acknowledgements. We gratefully thank the SouthTRAC coordination team, in particular DLR-FX for successfully conducting the field campaign, and local support from Argentina and Chile. For the successful campaign from Kathmandu, we thank the StratoClim coordination team as well as the Geophysica team, and local support from Nepal. The results are based on the efforts of all members of the GLORIA
305 team, including the technology institutes ZEA-1 and ZEA-2 at Forschungszentrum Jülich and the Institute for Data Processing and Electronics at the Karlsruhe Institute of Technology. The StratoClim campaign was supported by the European Community's Seventh Framework Programme (FP7/2007–2013) under grant no. 603557. The SouthTRAC measurement campaign was supported by the German Science

Foundation (Deutsche Forschungsgemeinschaft, DFG) under the Priority Program HALO SPP 1294. Within the HALO SPP this work was supported by project grant HO 4120/4-1. In addition the participating Helmholtz institutes contributed to the HALO operation costs based
310 on their programme-oriented funding We thank ECMWF for providing CAMS data. Contains Copernicus Atmosphere Monitoring Service Information 2023. Neither the European Commission nor ECMWF is responsible for any use that may be made of the information it contains. We thank AERIS for providing IASI NH$_3$ data, and we particularly appreciate helpful comments from Lieven Clarisse. We acknowledge support by the KIT-Publication Fund of the Karlsruhe Institute of Technology.

References

Appel, O., Köllner, F., Dragoneas, A., Hünig, A., Molleker, S., Schlager, H., Mahnke, C., Weigel, R., Port, M., Schulz, C., Drewnick, F., Vogel, B., Stroh, F., and Borrmann, S.: Chemical analysis of the Asian tropopause aerosol layer (ATAL) with emphasis on secondary aerosol particles using aircraft-based in situ aerosol mass spectrometry, Atmos. Chem. Phys., 22, 13 607–13 630, https://doi.org/10.5194/acp-22-13607-2022, 2022.

Basart, S., Benedictow, A., Bennouna, Y., Blechschmidt, A.-M., Chabrillat, S., Christophe, Y., Cuevas, E., Eskes, H. J., Hansen, K. M., Jorba, O., Kapsomenakis, J., Langerock, B., Pay, T., Richter, A., Sudarchikova, N., Schulz, M., Wagner, A., and Zerefos, C.: Upgrade verification note for the CAMS real-time global atmospheric composition service: Evaluation of the e-suite for the CAMS upgrade of July 2019, https://doi.org/10.24380/fcwq-yp50, 2019.

Beer, R., Shephard, M. W., Kulawik, S. S., Clough, S. A., Eldering, A., Bowman, K. W., Sander, S. P., Fisher, B. M., Payne, V. H., Luo, M., Osterman, G. B., and Worden, J. R.: First satellite observations of lower tropospheric ammonia and methanol, Geophysical Research Letters, 35, https://doi.org/10.1029/2008GL033642, 2008.

Bouwman, A. F., Lee, D. S., Asman, W. A. H., Dentener, F. J., van der Hoek, K. W., and Olivier, J. G. J.: A global high-resolution emission inventory for ammonia, Global Biogeochemical Cycles, 11, 561–587, https://doi.org/10.1029/97GB02266, 1997.

Clarisse, L., Shephard, M. W., Dentener, F., Hurtmans, D., Cady-Pereira, K., Karagulian, F., van Damme, M., Clerbaux, C., and Coheur, P.-F.: Satellite monitoring of ammonia: A case study of the San Joaquin Valley, Journal of Geophysical Research, 115, https://doi.org/10.1029/2009JD013291, 2010.

Clarisse, L., Franco, B., Van Damme, M., Di Gioacchino, T., Hadji-Lazaro, J., Whitburn, S., Noppen, L., Hurtmans, D., Clerbaux, C., and Coheur, P.: The IASI NH$_3$ version 4 product: averaging kernels and improved consistency, Atmospheric Measurement Techniques, 16, 5009–5028, https://doi.org/10.5194/amt-16-5009-2023, 2023.

Coheur, P.-F., Herbin, H., Clerbaux, C., Hurtmans, D., Wespes, C., Carleer, M., Turquety, S., Rinsland, C. P., Remedios, J., Hauglustaine, D., Boone, C. D., and Bernath, P. F.: ACE-FTS observation of a young biomass burning plume: First reported measurements of C_2H_4, C_3H_6O, H_2CO and PAN by infrared occultation from space, Atmospheric Chemistry and Physics, 7, 5437–5446, https://doi.org/10.5194/acp-7-5437-2007, 2007.

Eskes, H. J., Antonakaki, T., Basart, S., Benedictow, A., Blechschmidt, A.-M., Chabrillat, S., Christophe, Y., Clark, H., Cuevas, E., Hansen, K. M., Im, U., Kapsomenakis, J., Langerock, B., Richter, A., Schulz, M., Sudarchikova, N., Thouret, V., Wagner, A., and Zerefos, C.: Upgrade Verification Note for the CAMS Near-Real Time Global Atmospheric Composition Service, https://atmosphere.copernicus.eu/sites/default/files/2018-06/CAMS84_2015SC1_D84.3.2_201611_esuite_v1_0.pdf, 2016.

Eskes, H. J., Antonakaki, T., Basart, S., Benedictow, A., Blechschmidt, A.-M., Chabrillat, S., Christophe, Y., Clark, H., Cuevas, E., Hansen, K. M., Im, U., Kapsomenakis, J., Langerock, B., Petersen, K., Richter, A., Schulz, M., Sudarchikova, N., Thouret, V., Wagner, A., and Zerefos, C.: Upgrade Verification Note for the CAMS Near-Real Time Global Atmospheric Composition Service, https://atmosphere.copernicus.eu/sites/default/files/2018-06/CAMS84_2015SC2_D84.3.1.3_201706_esuite_v1_0.pdf, 2017.

Eskes, H. J., Basart, S., Benedictow, A., Bennouna, Y., Blechschmidt, A.-M., Chabrillat, S., Christophe, Y., Clark, H., Cuevas, E., Hansen, K. M., Im, U., Kapsomenakis, J., Langerock, B., Petersen, K., Schulz, M., Wagner, A., and Zerefos, C.: Upgrade Verification Note for the CAMS Near-Real Time Global Atmospheric Composition Service, https://atmosphere.copernicus.eu/sites/default/files/2019-02/CAMS84_2015SC2_D84.3.1.5_201802_esuite_v1_0.pdf, 2018.

350 Flemming, J., Huijnen, V., Arteta, J., Bechtold, P., Beljaars, A., Blechschmidt, A.-M., Diamantakis, M., Engelen, R. J., Gaudel, A., Inness, A., Jones, L., Josse, B., Katragkou, E., Marecal, V., Peuch, V.-H., Richter, A., Schultz, M. G., Stein, O., and Tsikerdekis, A.: Tropospheric chemistry in the Integrated Forecasting System of ECMWF, Geoscientific Model Development, 8, 975–1003, https://doi.org/10.5194/gmd-8-975-2015, 2015.

Friedl-Vallon, F., Gulde, T., Hase, F., Kleinert, A., Kulessa, T., Maucher, G., Neubert, T., Olschewski, F., Piesch, C., Preusse, P., Rongen,
355 H., Sartorius, C., Schneider, H., Schönfeld, A., Tan, V., Bayer, N., Blank, J., Dapp, R., Ebersoldt, A., Fischer, H., Graf, F., Guggenmoser, T., Höpfner, M., Kaufmann, M., Kretschmer, E., Latzko, T., Nordmeyer, H., Oelhaf, H., Orphal, J., Riese, M., Schardt, G., Schillings, J., Sha, M. K., Suminska-Ebersoldt, O., and Ungermann, J.: Instrument concept of the imaging Fourier transform spectrometer GLORIA, Atmospheric Measurement Techniques, 7, 3565–3577, https://doi.org/10.5194/amt-7-3565-2014, 2014.

Ge, C., Zhu, C., Francisco, J. S., Zeng, X. C., and Wang, J.: A molecular perspective for global modeling of upper atmospheric NH3 from
360 freezing clouds, Proceedings of the National Academy of Sciences, 115, 6147–6152, https://doi.org/10.1073/pnas.1719949115, 2018.

Granier, C., Bessagnet, B., Bond, T., D'Angiola, A., van der Denier Gon, H., Frost, G. J., Heil, A., Kaiser, J. W., Kinne, S., Klimont, Z., Kloster, S., Lamarque, J.-F., Liousse, C., Masui, T., Meleux, F., Mieville, A., Ohara, T., Raut, J.-C., Riahi, K., Schultz, M. G., Smith, S. J., Thompson, A., van Aardenne, J., van der Werf, G. R., and van Vuuren, D. P.: Evolution of anthropogenic and biomass burning emissions of air pollutants at global and regional scales during the 1980–2010 period, Climatic Change, 109, 163–190, https://doi.org/10.1007/s10584-
365 011-0154-1, 2011.

Guenther, A. B., Jiang, X., Heald, C. L., Sakulyanontvittaya, T., Duhl, T., Emmons, L. K., and Wang, X.: The Model of Emissions of Gases and Aerosols from Nature version 2.1 (MEGAN2.1): an extended and updated framework for modeling biogenic emissions, Geoscientific Model Development, 5, 1471–1492, https://doi.org/10.5194/gmd-5-1471-2012, 2012.

Hegg, D. A., Radke, L. F., Hobbs, P. V., and Riggan, P. J.: Ammonia emissions from biomass burning, Geophysical Research Letters, 15,
370 335–337, https://doi.org/10.1029/gl015i004p00335, 1988.

Huijnen, V., Williams, J., Van Weele, M., Van Noije, T., Krol, M., Dentener, F., Segers, A., Houweling, S., Peters, W., De Laat, J., Boersma, F., Bergamaschi, P., Van Velthoven, P., Le Sager, P., Eskes, H., Alkemade, F., Scheele, R., Nédélec, P., and Pätz, H.-W.: The global chemistry transport model TM5: description and evaluation of the tropospheric chemistry version 3.0, Geoscientific Model Development, 3, 445–473, https://doi.org/10.5194/gmd-3-445-2010, 2010.

375 Höpfner, M., Volkamer, R., Grabowski, U., Grutter, M., Orphal, J., Stiller, G., Clarmann, T. V., and Wetzel, G.: First detection of ammonia (NH$_3$) in the Asian summer monsoon upper troposphere, Atmospheric Chemistry and Physics, 16, 14 357–14 369, https://doi.org/10.5194/acp-16-14357-2016, 2016.

Höpfner, M., Ungermann, J., Borrmann, S., Wagner, R., Spang, R., Riese, M., Stiller, G., Appel, O., Batenburg, A. M., Bucci, S., Cairo, F., Dragoneas, A., Friedl-Vallon, F., Hünig, A., Johansson, S., Krasauskas, L., Legras, B., Leisner, T., Mahnke, C., Möhler, O., Molleker,
380 S., Müller, R., Neubert, T., Orphal, J., Preusse, P., Rex, M., Saathoff, H., Stroh, F., Weigel, R., and Wohltmann, I.: Ammonium nitrate particles formed in upper troposphere from ground ammonia sources during Asian monsoons, Nature Geoscience, 12, 608–612, https://doi.org/10.1038/s41561-019-0385-8, 2019.

Inness, A., Flemming, J., Heue, K.-P., Lerot, C., Loyola, D., Ribas, R., Valks, P., van Roozendael, M., Xu, J., and Zimmer, W.: Monitoring and assimilation tests with TROPOMI data in the CAMS system: Near-real-time total column ozone, Atmospheric Chemistry and Physics,
385 19, 3939–3962, https://doi.org/10.5194/acp-19-3939-2019, 2019.

Johansson, S., Woiwode, W., Höpfner, M., Friedl-Vallon, F., Kleinert, A., Kretschmer, E., Latzko, T., Orphal, J., Preusse, P., Ungermann, J., Santee, M. L., Jurkat-Witschas, T., Marsing, A., Voigt, C., Giez, A., Krämer, M., Rolf, C., Zahn, A., Engel, A., Sinnhuber, B.-M.,

and Oelhaf, H.: Airborne limb-imaging measurements of temperature, HNO_3, O_3, $ClONO_2$, H_2O and CFC-12 during the Arctic winter 2015/2016: Characterization, in situ validation and comparison to Aura/MLS, Atmospheric Measurement Techniques, 11, 4737–4756, https://doi.org/10.5194/amt-11-4737-2018, 2018.

Johansson, S., Höpfner, M., Kirner, O., Wohltmann, I., Bucci, S., Legras, B., Friedl-Vallon, F., Glatthor, N., Kretschmer, E., Ungermann, J., and Wetzel, G.: Pollution trace gas distributions and their transport in the Asian monsoon upper troposphere and lowermost stratosphere during the StratoClim campaign 2017, Atmospheric Chemistry and Physics, 20, 14695–14715, https://doi.org/10.5194/acp-20-14695-2020, 2020.

Johansson, S., Wetzel, G., Friedl-Vallon, F., Glatthor, N., Höpfner, M., Kleinert, A., Neubert, T., Sinnhuber, B.-M., and Ungermann, J.: Biomass burning pollution in the South Atlantic upper troposphere: GLORIA trace gas observations and evaluation of the CAMS model, Atmospheric Chemistry and Physics, 22, 3675–3691, https://doi.org/10.5194/acp-22-3675-2022, 2022.

Kaiser, J. W., Heil, A., Andreae, M. O., Benedetti, A., Chubarova, N., Jones, L., Morcrette, J.-J., Razinger, M., Schultz, M. G., Suttie, M., and van der Werf, G. R.: Biomass burning emissions estimated with a global fire assimilation system based on observed fire radiative power, Biogeosciences, 9, 527–554, https://doi.org/10.5194/bg-9-527-2012, 2012.

Kirkby, J., Amorim, A., Baltensperger, U., Carslaw, K. S., Christoudias, T., Curtius, J., Donahue, N. M., Haddad, I. E., Flagan, R. C., Gordon, H., Hansel, A., Harder, H., Junninen, H., Kulmala, M., Kürten, A., Laaksonen, A., Lehtipalo, K., Lelieveld, J., Möhler, O., Riipinen, I., Stratmann, F., Tomé, A., Virtanen, A., Volkamer, R., Winkler, P. M., and Worsnop, D. R.: Atmospheric new particle formation from the CERN CLOUD experiment, Nat. Geosci., 16, 948–957, https://doi.org/10.1038/s41561-023-01305-0, 2023.

Kleinert, A., Friedl-Vallon, F., Guggenmoser, T., Höpfner, M., Neubert, T., Ribalda, R., Sha, M. K., Ungermann, J., Blank, J., Ebersoldt, A., Kretschmer, E., Latzko, T., Oelhaf, H., Olschewski, F., and Preusse, P.: Level 0 to 1 processing of the imaging Fourier transform spectrometer GLORIA: Generation of radiometrically and spectrally calibrated spectra, Atmospheric Measurement Techniques, 7, 4167–4184, https://doi.org/10.5194/amt-7-4167-2014, 2014.

Morcrette, J., Boucher, O., Jones, L., Salmond, D., Bechtold, P., Beljaars, A., Benedetti, A., Bonet, A., Kaiser, J. W., Razinger, M., Schulz, M., Serrar, S., Simmons, A. J., Sofiev, M., Suttie, M., Tompkins, A. M., and Untch, A.: Aerosol analysis and forecast in the European Centre for Medium-Range Weather Forecasts Integrated Forecast System: Forward modeling, Journal of Geophysical Research: Atmospheres, 114, D06206, https://doi.org/10.1029/2008JD011235, 2009.

Nowak, J. B., Neuman, J. A., Bahreini, R., Brock, C. A., Middlebrook, A. M., Wollny, A. G., Holloway, J. S., Peischl, J., Ryerson, T. B., and Fehsenfeld, F. C.: Airborne observations of ammonia and ammonium nitrate formation over Houston, Texas, Journal of Geophysical Research, 115, https://doi.org/10.1029/2010JD014195, 2010.

Riese, M., Oelhaf, H., Preusse, P., Blank, J., Ern, M., Friedl-Vallon, F., Fischer, H., Guggenmoser, T., Höpfner, M., Hoor, P., Kaufmann, M., Orphal, J., Plöger, F., Spang, R., Suminska-Ebersoldt, O., Ungermann, J., Vogel, B., and Woiwode, W.: Gimballed Limb Observer for Radiance Imaging of the Atmosphere (GLORIA) scientific objectives, Atmospheric Measurement Techniques, 7, 1915–1928, https://doi.org/10.5194/amt-7-1915-2014, 2014.

Rémy, S., Metzger, S., Huijnen, V., Williams, J. E., and Flemming, J.: An improved representation of aerosol acidity in the ECMWF IFS-COMPO 49R1 through the integration of EQSAM4Climv12, EGUsphere, 2024, 1–41, https://doi.org/10.5194/egusphere-2023-3072, 2024.

Shephard, M. W. and Cady-Pereira, K. E.: Cross-track Infrared Sounder (CrIS) satellite observations of tropospheric ammonia, Atmospheric Measurement Techniques, 8, 1323–1336, https://doi.org/10.5194/amt-8-1323-2015, 2015.

Sinnhuber, B.-M., Chipperfield, M., Errera, Q., Friedl-Vallon, F., Funke, B., Hoffmann, A., Malavart, A., Osprey, S., Polichtchouk, I., Preusse, P., Raspolini, P., Schüttemeyer, D., Ungermann, J., Verronen, P., and Walker, K.: Changing-Atmosphere Infra-Red Tomography Explorer, https://www.cairt.eu/, accessed: 2023-11-28, 2023.

Spang, R., Remedios, J. J., and Brarkley, M. P.: Colour indices for the detection and differentiation of cloud types in infra-red limb emission spectra, Advances in Space Research, 33, 1041–1047, https://doi.org/10.1016/S0273-1177(03)00585-4, publisher: Pergamon, 2004.

Stiller, G. P., ed.: The Karlsruhe Optimized and Precise Radiative transfer Algorithm (KOPRA), vol. FZKA 6487 of *Wissenschaftliche Berichte*, Forschungszentrum Karlsruhe, 2000.

Szopa, S., Naik, V., Adhikary, B., Artaxo, P., Berntsen, T. K., Collins, W. D., Fuzzi, S., Gallardo, L., Kiendler-Scharr, A., and Klimont, Z.: Short-lived Climate Forcers, in: Climate Change 2021 – The Physical Science Basis, edited by Change, I. P. o. C., pp. 817–922, Cambridge University Press, Cambridge, United Kingdom and New York, NY, US, 2021.

Tomsche, L., Piel, F., Mikoviny, T., Nielsen, C. J., Guo, H., Campuzano-Jost, P., Nault, B. A., Schueneman, M. K., Jimenez, J. L., Halliday, H., Diskin, G., DiGangi, J. P., Nowak, J. B., Wiggins, E. B., Gargulinski, E., Soja, A. J., and Wisthaler, A.: Measurement report: Emission factors of NH_3 and NH_x for wildfires and agricultural fires in the United States, Atmospheric Chemistry and Physics, 23, 2331–2343, https://doi.org/10.5194/acp-23-2331-2023, 2023.

Ungermann, J., Kleinert, A., Maucher, G., Bartolomé, I., Friedl-Vallon, F., Johansson, S., Krasauskas, L., and Neubert, T.: Quantification and mitigation of the instrument effects and uncertainties of the airborne limb imaging FTIR GLORIA, Atmospheric Measurement Techniques, 15, 2503–2530, https://doi.org/10.5194/amt-15-2503-2022, 2022.

van Damme, M., Clarisse, L., Dammers, E., Liu, X., Nowak, J. B., Clerbaux, C., Flechard, C. R., Galy-Lacaux, C., Xu, W., Neuman, J. A., Tang, Y. S., Sutton, M. A., Erisman, J. W., and Coheur, P. F.: Towards validation of ammonia (NH_3) measurements from the IASI satellite, Atmospheric Measurement Techniques, 8, 1575–1591, https://doi.org/10.5194/amt-8-1575-2015, 2015.

von Bobrutzki, K., Braban, C. F., Famulari, D., Jones, S. K., Blackall, T., Smith, T. E. L., Blom, M., Coe, H., Gallagher, M., Ghalaieny, M., McGillen, M. R., Percival, C. J., Whitehead, J. D., Ellis, R., Murphy, J., Mohacsi, A., Pogany, A., Junninen, H., Rantanen, S., Sutton, M. A., and Nemitz, E.: Field inter-comparison of eleven atmospheric ammonia measurement techniques, Atmospheric Measurement Techniques, 3, 91–112, https://doi.org/10.5194/amt-3-91-2010, 2010.

Wagner, R., Bertozzi, B., Höpfner, M., Höhler, K., Möhler, O., Saathoff, H., and Leisner, T.: Solid Ammonium Nitrate Aerosols as Efficient Ice Nucleating Particles at Cirrus Temperatures, Journal of Geophysical Research: Atmospheres, 125, https://doi.org/10.1029/2019JD032248, 2020.

Wang, Y., Ma, Y.-F., Eskes, H., Inness, A., Flemming, J., and Brasseur, G. P.: Evaluation of the CAMS global atmospheric trace gas reanalysis 2003–2016 using aircraft campaign observations, Atmospheric Chemistry and Physics, 20, 4493–4521, https://doi.org/10.5194/acp-20-4493-2020, 2020.

Warner, J. X., Wei, Z., Strow, L. L., Dickerson, R. R., and Nowak, J. B.: The global tropospheric ammonia distribution as seen in the 13-year AIRS measurement record, Atmospheric Chemistry and Physics, 16, 5467–5479, https://doi.org/10.5194/acp-16-5467-2016, 2016.

Wetzel, G., Friedl-Vallon, F., Glatthor, N., Grooß, J.-U., Gulde, T., Höpfner, M., Johansson, S., Khosrawi, F., Kirner, O., Kleinert, A., Kretschmer, E., Maucher, G., Nordmeyer, H., Oelhaf, H., Orphal, J., Piesch, C., Sinnhuber, B.-M., Ungermann, J., and Vogel, B.: Pollution trace gases C_2H_6, C_2H_2, HCOOH, and PAN in the North Atlantic UTLS: observations and simulations, Atmospheric Chemistry and Physics, 21, 8213–8232, https://doi.org/10.5194/acp-21-8213-2021, 2021.

Ziereis, H. and Arnold, F.: Gaseous ammonia and ammonium ions in the free troposphere, Nature, 321, 503–505, https://doi.org/10.1038/321503a0, 1986.